MedChemComm

Accepted Manuscript

This article can be cited before page numbers have been issued, to do this please use: S. Kumari, J. Chowdhary, M. Sikka, P. Verma, P. Jha, A. K. Mishra, D. Saluja and M. Chopra, *Med. Chem. Commun.*, 2017, DOI: 10.1039/C7MD00171A.

ROYAL SOCIETY OF CHEMISTRY

rsc.li/medchemcomm

View Article Online
DOI: 10.1039/C7MD00171A

MedChemComm

ARTICLE

Received 00th January 20xx,
Accepted 00th January 20xx

DOI: 10.1039/x0xx00000x

www.rsc.org/

Identification of Potent Cholecystokinin-B Receptor Antagonists: Synthesis, Molecular Modeling and anti-cancer activity against Pancreatic Cancer Cells.

Saroj Kumari[†], Joyita Chowdhury[a,†], Manisha Sikka[a], Priyanka Verma[a], Prakash Jha[a], Anil K. Mishra[b], Daman Saluja[a] and Madhu Chopra*[a]

* Corresponding Author

[†] These authors contributed equally to the work

a. Laboratory of Anticancer Drug Development, Dr. B. R. Ambedkar Center for Biomedical Research, University of Delhi, Delhi 110007, India
E-mail:mchopradu@gmail.com, mchopra@acbr.du.ac.in

b. Institute of Nuclear Medicine and Allied Sciences, Brig. S. K. Majumdar Road, Delhi 110054, India

Abstract: Advanced malignant stage of pancreatic cancer has poor prognosis and very few treatment strategies are available. Pancreatic cancer is known to possess unique growth-related receptors that when activated stimulate tumour proliferation. Gastrin and its related peptide cholecystokinin (CCK) are also significantly involved with growth of this cancer type as well as other malignancies through activation of the cholecystokinin-B receptor (CCK-BR). New treatment strategies with CCK-BR antagonists are being suggested that suppress the growth promoting effects of gastrin. In this paper, we report development of two series of quinazolinonederivatives incorporating hydrazinecarbothioamide (compounds 3a-g) and hydrazino group (Compounds 4a-e) as linkers for developing CCK-BR antagonists. The affinities of the compounds were determined using docking into CCK-BR homology modeled structure. The compounds were tested for *in vitro* CCK-BR binding and gastric acid secretion in an isolated lumen-perfused mouse stomach assay. The compounds exhibited CCK-BR binding activity (IC_{50}) in the range of 0.2 – 975 nM and showed good gastric acid secretion inhibitory activity. Molecular modeling of the compounds was done and pharmacophore mapping results showed good prediction *of in vitro* activity which correlated well with the experimental antagonistic activity. The compounds were further tested for their cytotoxicity on CCK-BR expressing pancreatic cancer cells. The results of the study provided two potent CCK-BR antagonists which also possess good to moderate growth inhibitory activities against pancreatic cancer cells.

View Article Online
DOI: 10.1039/C7MD00171A
ARTICLE
Journal Name

Introduction

Pancreatic cancer in advanced malignant stages has a poor prognosis[1,2] and currently available therapeutic modalities have not markedly improved survival rate[3]. Pancreatic cancer is the twelfth most common cancer in the world. It is suggested that this malignancy will surpass colon and breast cancer in the next decade with current rate of rise in incidence and therefore will become second leading cause of cancer related deaths in the USA.[4]

Gastrointestinal peptides such as gastrin and cholecystokinin (CCK) have been reported to have growth stimulatory effects on pancreatic cancer and the receptor for these peptides is markedly over-expressed in pancreatic cancer[5,6]. These peptide hormones activate their receptors (CCK in this case) in pancreatic cancer through induction of AKT pathway[7] resulting in cell proliferation. There is sufficient evidence that CCK-BR pathway is a key driver of pancreatic carcinogenesis, pancreatic cancer and other malignancies[8].

Several studies have reported presence of a mutated form of CCK-BR containing the translated 4th intron, termed as CCK-C or CCK- cancer receptor (CCK-CR) in pancreatic cancer[9]. Studies suggest that these additional 69 amino acids of the CCK-C receptor render the receptor constitutively active where it induces proliferation even in the absence of gastrin[10]. Thus blocking this receptor in pancreatic cancer becomes even more important to slow down the proliferation. Moreover, it is also interested to know that both CCK-BR and its splice variant CCK-CR bind to CCK and gastrin[11].

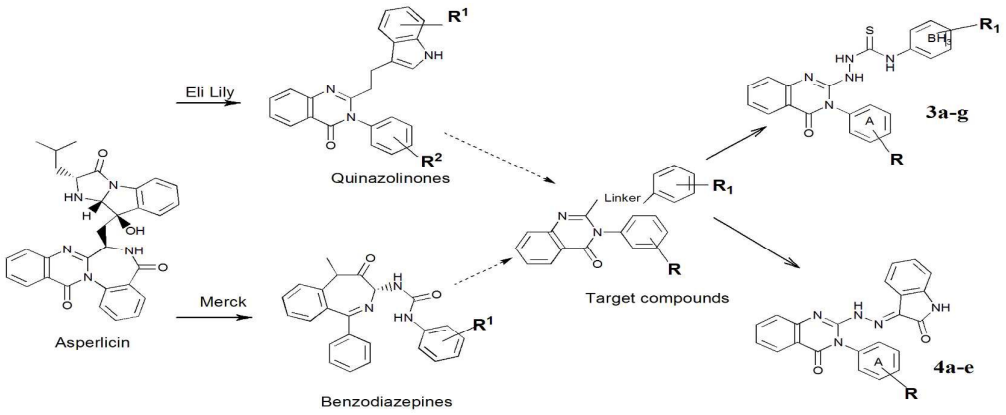

Scheme 1: Design of CCK-BR antagonists

Several treatment strategies are currently being exploited to interrupt the CCK/gastrin: CCK-receptor (CCK-R) pathway in cancer. In the last decade, several highly selective CCK-A and CCK-B receptor antagonists have been developed[12]. This includes use of oligonucleotides to gastrin[13], gastrin specific antibodies[14], as well as using gastrin vaccine, "Gastrimmune", or G17DT. A randomized placebo controlled study using vaccine therapy demonstrated a significant survival benefit in pancreatic cancer patients that elicited neutralizing antibodies towards gastrin response to vaccination with G17DT.

In addition to above strategies; studies have been reported to stop the CCK-R activation through use of specific antagonists though an initial clinical trial done with MK-329, a selective CCK-A receptor antagonist failed[15,16]. Since it is well known fact that the CCK-BR subtype is the primary type of receptor that mediates the cancer growth in pancreatic cancer in humans, the research focus has thus been shifted to use of CCK-BR specific antagonists. E.g. a highly selective CCK-BR antagonist, netazepide (YF476) was used to treat patients with type 1 gastrin carcinoid tumour[17] and further studies are needed using more potent and selective antagonists in pancreatic cancer. A phase Ib/IIa clinical trial is underway to evaluate CCKBR antagonist Z-360 in combination with gemcitabine (a cytosine analogue and antineoplastic agent, used as an anti-cancer chemotherapy drug) in patients with advanced pancreatic cancer[18]. In recent years also, there is a study on Pancreatic ductal adenocarcinomas (PDACs) which are known to constitutively express the CCKBR, using DNA aptamer AP1153[19], and it is anticipated that

View Article Online
DOI: 10.1039/C7MD00171A

new *CCKBR* AP-targeted nanocarriers will have a broad capability to deliver imaging agents or therapeutic cargos specifically to PDAC cells with minimal off-target effects.

There is dire need for novel therapeutic agents which can target the gastrin: CCK-B–receptor pathways[20] which may help improve survival of advanced gastric cancer. All above studies provide sufficient evidence that new treatment regimens with CCK-BR antagonists could suppress the growth promoting effects of gastrin. In the present work, we are demonstrating synthesis, docking and *in vitro* evaluation of quinazolinone derivatives as potent CCK-BR antagonists and their Cytotoxicity evaluation against pancreatic cancer cells (MiaPaca-2).

There are several distinct chemical classes of CCK-BR antagonists that have previously been identified through drug discovery programs. These include benzodiazepine-based compounds (**L-365,260**), (**YM022**), and (Y**F476**); peptoids (**PD-134,308**)] and indole (**JB93182**)[21]. However, despite the variety of CCK-BR targeted ligands, very few compounds are currently available for clinical use. This may be because many compounds in this class have been associated with poor or variable pharmacokinetics, both with respect to gastrointestinal absorption and blood-brain permeability[21]. Since our compounds are targeted against pancreatic cancer, poor blood–brain permeability could be a good tool to distinguish between peripheral and central effects of CCKBR antagonism as already reported in case of **S-0509**[22], which is currently at Phase I clinical trials for gastric secretion disorders. Hence, there is a need to design new CCK-BR antagonists.

Our lab is developing CCK-BR specific antagonists which have been designed by taking lead from naturally occurring compound, Asperlicin, a weak and non-selective CCK ligand. In a previous communication, we have shown design and synthesis of one such potent antagonist linked to fluorescein moiety and used it as imaging agent to study receptor trafficking in CCK-BR positive cells[23]. In another communication we have shown synthesis and *in vivo* biological activity of another quinazolinone derivative[24]. We have shown that the two key moieties, a quinazolinone ring and an aryl ring linked with a proper linker are crucial for CCK-BR binding. Continuing our efforts further, in the present paper, we report synthesis, biological evaluation of several derivatives of these two series of compounds. We decided to explore the effect of two types of linkers. One series of compounds **(3a-g)** were prepared by incorporating hydrazine carbothioamide –NHNH-CS-NH- as linker between the quinazolinone and the aryl moiety and the other **(4a-e)** were synthesized by keeping hydrazino group (=N-NH-) as linker between the quinazolinone and the indanone. (Scheme 1) and the effect of substitutions in aryl ring was studied.

Results and Discussion

Chemistry

The compounds described in this paper were prepared according to Scheme 2 incorporating either hydrazinecarbothioamide **(Compounds 3a-g)** or a hydrazine linker **(Compounds 4a-e)**. In the former series, quinazolinone ring was prepared by one pot reaction of anthranilic acid with phenylisothiocyanates in glacial acetic

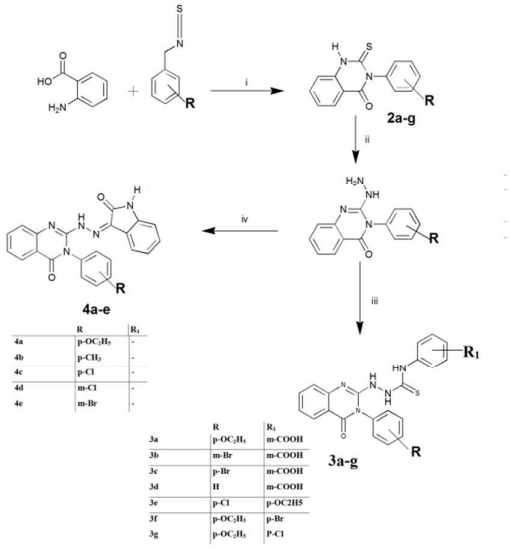

	R	R_1
4a	p-OC_2H_5	-
4b	p-CH_3	-
4c	p-Cl	-
4d	m-Cl	-
4e	m-Br	-

	R	R_1
3a	p-OC_2H_5	m-COOH
3b	m-Br	m-COOH
3c	p-Br	m-COOH
3d	H	m-COOH
3e	p-Cl	p-OC2H5
3f	p-OC_2H_5	p-Br
3g	p-OC_2H_5	P-Cl

Scheme 2: Scheme for the synthesis of Quinazolinone Derivatives (i) ACOH, reflux (ii) anhy.hydrazine, abs. EtOH (iii) isothiocyanates, anhy. DMF, 110 ^{o}C (iv) isatin, abs. EtOH, reflux.

acid under reflux conditions. The hydrazone derivatives **(compound 2a-g)** were obtained by treatment of the thioxoquinazolinones **(compounds 1a-f)** with excess of anhydrous hydrazine in refluxing absolute ethanol. The isothiocyanates which were not commercially available were prepared by the standard methodology reported in the literature.

The hydrazinoquinazolinones **(compounds 2a-g)** were treated either with isothiocyanates or isatin to provide compounds **(3a-g)** and **(4a-e),** respectively. One such compound **3a** was attached with fluorescein in our previous communication and has been shown to have affinity in nM range and we successfully used it as fluorescence probe to image CCK-BR positive cells[23]. In order to improve pharmacokinetic properties we are reporting synthesis of derivative of these series of compounds and their antagonistic activities. The cytotoxic activities of these compounds have also been evaluated against CCK-BR expressing human pancraetic cancer cells (MiaPaca-2).

Molecular Modeling

Pharmacophore mapping and prediction of activity

In a previous paper, we developed pharmacophore model based on six chemically diverse series of compounds taken from literature[25]. The pharmacophore model was validated on a test series of compounds taken from literature and resulted in good prediction of antagonistic activities. The basic features essential for CCK-BR antagonistic activities identified in the paper were used here for the synthesis of quinazolinone derivatives. The pharmacophore[25] was used in present work to predict the antagonistic activities of the synthesized compounds which correlated very well with the *in-vitro* results. All the newly synthesized compounds gave a pharmacophore fit value in the range of 7.83 – 5.33 with predicted activities in the range of 0.82 nM – 257 nM upon mapping to the features of the pharmacophore model. (Table1).

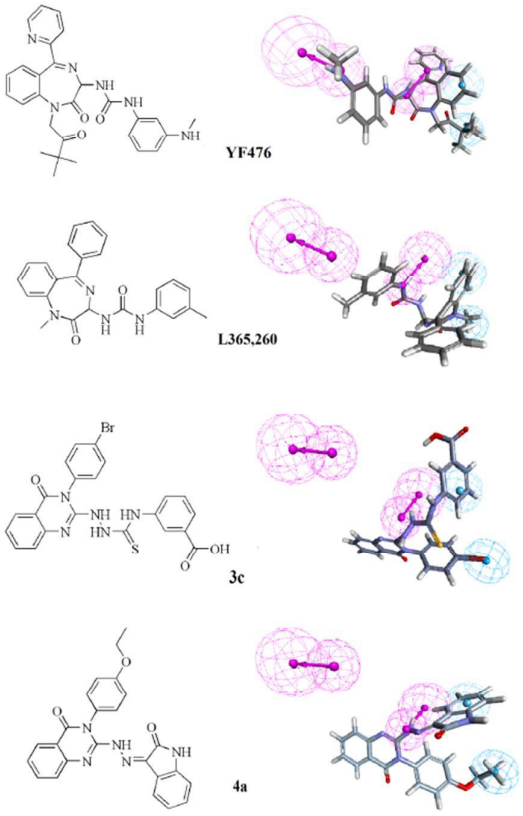

Figure1. Mapping of the CCKBR antagonists onto the pharmacophore model (hypothesis 1). The blue contour represents the HY-ALI features, the cyan contour represents HY-AR features, and the dark pink contour represents the HBD features.

View Article Online
DOI: 10.1039/C7MD00171A

Comp. no.	Substitution		Potential energy kcalmol^{-1}	Fit value	Features mapped	Estimated activity IC_{50} (nM)	Actual Activity IC_{50} in nM	Activity Scale (Estimated)	Activity scale (Actual)	CDOCKER ENERGY kcalmol^{-1}	CDOCKER INTERACTION ENERGY kcalmol^{-1}	Gastric acid secretion inhibition (%) at 100 nM	Cytotoxicity Evaluation IC_{50} (μM)
YF476	-	-	-41.44	9.864	1111	0.0076	0.10[a]	+++	+++	-22.52	-37.96	ND	ND
L365,260	-	-	0.1167	7.946	1011	0.0636	5.2[a]	+++	+++	-19.09	-33.84	ND	0.0018
	R	R_1											
3a	p-OC_2H_5	m-COOH	-67.816	7.75	1011	0.985	0.66	+++	+++	-19.33	-36.16	58	280
3b	m-Br	m-COOH	-67.18	7.49	1011	1.74	8.64	+++	+++	-18.38	-37.46	62	150
3c	p-Br	m-COOH	-66.109	7.17	1011	3.79	0.2001	+++	+++	-17.73	-37.85	39	200
3d	H	m-COOH	-65.37	5.33	1001	257	975.4	+	+	-20.87	-35.01	48 at 1 μM	180
3e	p-Cl	p-OC2H5	-44.5	7.72	1011	1.05	9.715	+++	+++	-17.91	-37.05	53	80
3f	p-OC_2H_5	p-Br	-43.528	7.81	1011	0.863	2.005	+++	+++	-21.37	-34.33	39	10
3g	p-OC_2H_5	P-Cl	-44.29	7.83	1011	0.82	11.48	+++	+++	-16.09	-37.12	58	250
4a	p-OC_2H_5	-	48.58	6.78	1011	9.37	17.36	+++	+++	4.78	-31	48	80
4b	p-CH_3	-	32.48	5.48	1011	185.5	56.49	++	++	2.26	-28.26	67 at 300 nM	10
4c	p-Cl	-	33.82	5.55	1011	158.2	ND	++	ND	5.3	-33.43	58	100
4d	m-Cl	-	35.85	5.74	1011	100.8	384.2	++	+	4.5	-28.41	58	92
4e	m-Br	-	34.84	6.38	1011	23.1	19.46	++	+++	1.9	-35.36	62	200

Table 1: CCKBR Antagonists 3a-g and 4a-e produced via Scheme 1.

[a]activities were taken from literature determined through similar assay *(J. Med. Chem.*, **1993**, *36* (26), pp 4276–4292&G. S. Baldwin, *PNAS*, 1994, **91**, 7593–7597)

[b]Activity scale: +++ (0-20nM, highly active), ++ (30-200 nM, moderately active), + (>200 nM, poorly active) *(J. Chem. Inf. Model.*, 2005, **45**, 1934–1942))

We also compared the fit values and estimated activities with known CCK-BR antagonists **YF476** and **L365, 260**. The compound **YF476**, a highly potent and orally active CCK-BR antagonist showed a fit value of 9.864 with an estimated activity of 0.0076 nM and mapped to all the four features and has a reported IC_{50} of 0.10 nM using a similar assay[26]. Another compound, **L-365,260**, showed a fit value of 7.946 and an estimated activity of 0.06367 nM (Actual activity, IC_{50} = 3.8nM) mapped to three features of thepharmacophore[27]. As we have shown earlier[25]; a fit value from 6 – 8 bits suggests that a compound could be highly active and those with fit value less than 6 bits might be moderately active or weakly active compounds. The compounds developed in this study showed high (Fit value 7.83, 0.82 nM as estimated activity) to moderate activity (Fit value 5.33, 257 nM as estimated activity) and correlated well with the corresponding actual activities (Table 1). The highly active compounds mapped similar to the potent compound **L-365,260** (Figure. 1).

Homology Modeling of CCK-BR

The sequence alignment of human CCK-BR (ID: P32239) and the template human A2A adenosine receptor was generated using Clustal W and manually adjusted to avoid the insertions and deletions in the conserved transmembrane regions. The sequence similarity and sequence identity of the aligned sequence are 19.2 and 36.3% respectively. The best modeled structure with the least DOPE score[28] (38262.156250) and PDF energy score[28] (-8161.8936 kcalmol^{-1}) was selected for molecular dynamics simulations

Molecular dynamics simulation and validation

Molecular dynamics (MD) simulations were performed to improve the structure of CCK-BR and to study its bio-physical properties. The MD simulation results show that the model clearly diverged and the conserved disulphide bridge remained stable throughout the simulations. The root mean square deviation (RMSD) of less than 1 nm was obtained in the plot of backbone atoms.

The potential energy analysed during the 4ns molecular dynamics simulation showed that the molecular system is stabilized and remained stable throughout the molecular dynamics simulations with the average of potential energy stabilized around -3.47 × 10^4 kJ/mol.

View Article Online
DOI: 10.1039/C7MD00171A
ARTICLE
Journal Name

Model Evaluation

The model was evaluated using verify 3D score, ERRAT score and favourable residues in Ramachandran plot (*See Supplementary material*). The verify 3D score of simulated protein, was 77.83, which is greater than expected low score as well as the verify score of the modelled protein before simulations. The phi and psi angles of the receptor were verified by Ramachandran plot which showed 81.8 % residues falling in the favoured region, 99% within additionally allowed region and none of the binding site residue in the disallowed region. The ERRAT score was 95.68 suggesting 'very good quality' of the modelled protein structure.

Active Site Prediction

After obtaining the final model, active sites of the protein were predicted using discovery studio based on receptor cavity method and further modified manually using the active site residues namely Asn353A$^{6.55}$, Arg356A$^{6.58}$(TM6), His207(EL2), and Tyr189A$^{4.60}$(TM4) which are know to be involved in CCK-BR antagonism for non-peptide antagonists through site directed mutagenesis and docking Studies reported earlier[29,30].

Molecular Docking

The energy minimised structures of the compounds in the study were docked into the active site of the modeled CCK-BR structure. **L365,260 and YF476** both, on being docked intothe modelled CCK-BR active site revealed H-bond interactions with Arg356A$^{6.58}$ (**L365,260**), Asn353A$^{6.55}$and Arg356A$^{6.58}$ (**YF476**). Both the compounds showed π – positive charge interaction with Arg356A$^{6.58}$ through their respective aromatic rings (Figure 2). **YF476** showed hydrophobic alkyl interaction with Arg356A$^{6.58}$ in addition to π–Sulphur bond with Met117 (EL1) and π–Alkyl hydrophobic bond with Ile375A$^{7.38}$, Leu113A$^{2.63}$ and Pro114A$^{2.64}$. In the case of **L365, 260**, the benzodiazepine core also showed π–Alkyl hydrophobic bond with His364 (EL3) and Ala366 (EL3) and Hydrophobic – Alkyl interaction with Ile375A$^{7.38}$. Both the ligands were further stabilized by common van der Waals interactions to residues His376A$^{7.39}$, Pro114A$^{2.64}$, Ile375A$^{7.38}$ and Ala352A$^{6.54}$.

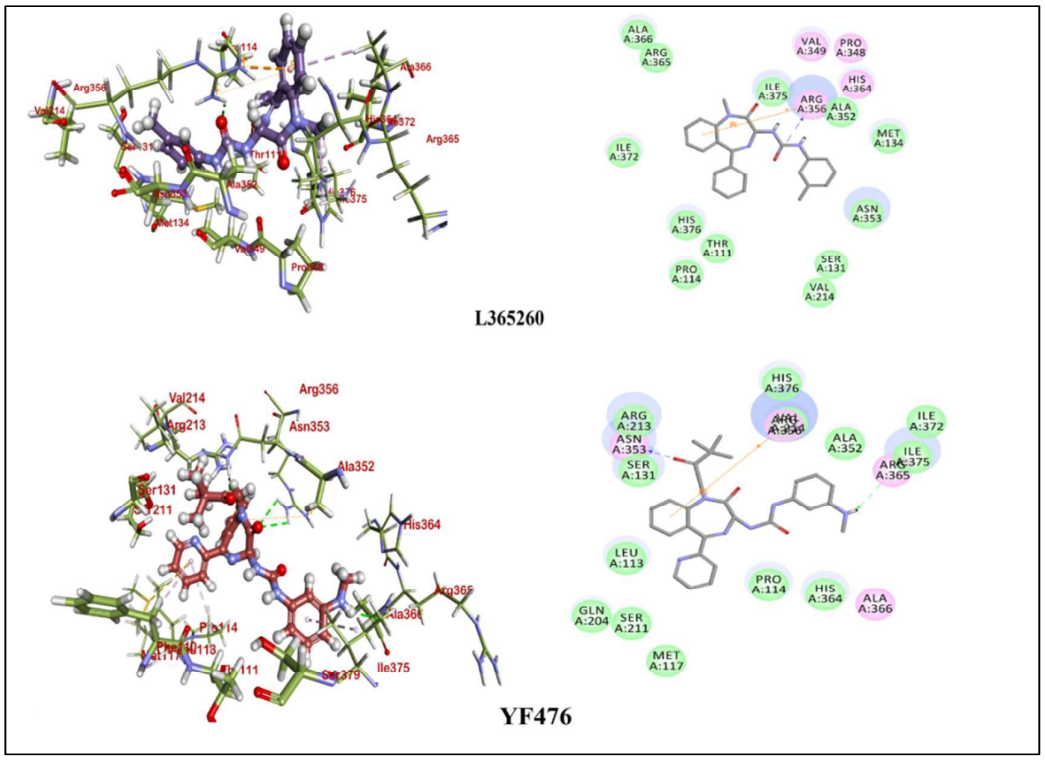

Figure 2: Docked structures of L365,260 and YF476, into the homology modelled CCK-B structure.

View Article Online
DOI: 10.1039/C7MD00171A

Similarly, the common binding pocket for all our synthesized ligands is composed of residues Arg356A$^{6.58}$, Asn353A$^{6.55}$, Leu113A$^{2.63}$, Pro114A$^{2.64}$, His376A$^{7.39}$, Ser379A$^{7.42}$, Thr111A$^{2.61}$, Ile375A$^{7.38}$and Val349A$^{6.51}$, which are in the distance interval of 1.5 to 10 Å from the closest ligand atom. In addition to many hydrophobic contacts that contributed the most to the binding, ionic and hydrogen bonds could also be identified. The most active compound **3c** showed π– bonding of quinazolinone core with Arg356A$^{6.58}$, similar to that shown by **L365, 260** and **YF476** (discussed above). **3c** also interacted through hydrophobic π– π T-shaped bond with His376A$^{7.39}$and two H – bonds with Asn353A$^{6.55}$. The residues, namely Leu113A$^{2.63}$, Pro114A$^{2.64}$ and Arg356A$^{6.58}$ were also found to form π– alkyl hydrophobic bonds with **3c**. Similar to **YF476** and **L365, 260**, it also showed van der Waals interactions with residues Leu113A$^{2.63}$, Pro114A$^{2.64}$, and Ile375A$^{7.38}$ (Figure3). The compound **3f** also showed π– bonding of quinazolinone core with Arg356A$^{6.58}$ as seen in **L365, 260** and **YF476 along with H-bond with Asn353A$^{6.55.}$** It also showed π– alkyl hydrophobic bonds with His376A$^{7.39}$ and Pro114A$^{2.64}$ were further stabilised by hydrophobic-alkyl bonds with Ile372 and Met134.

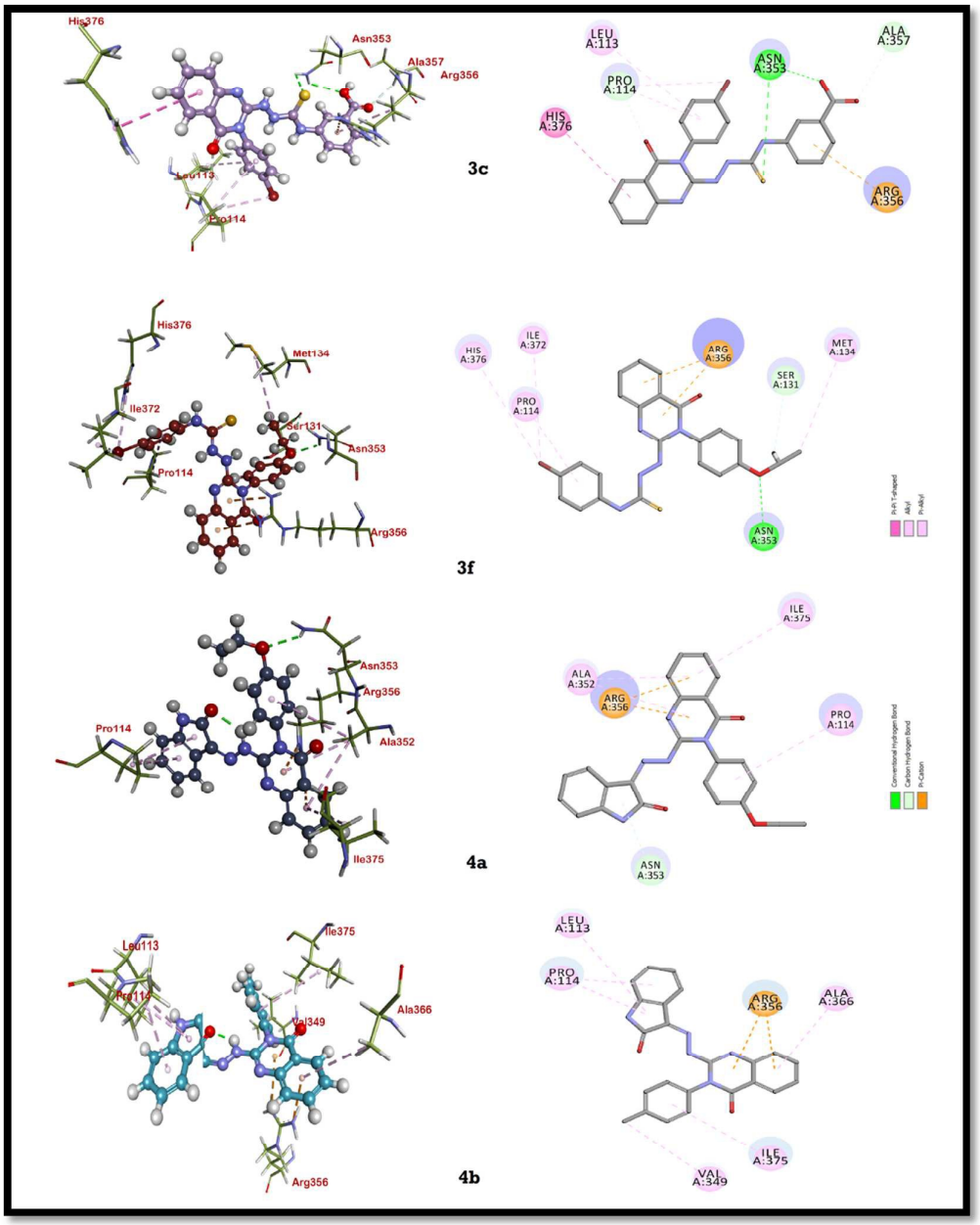

Figure 3 :Docked structures of 3a, 3f, 4a and 4b into the homology modelled CCK-B structure.

View Article Online
DOI: 10.1039/C7MD00171A
ARTICLE Journal Name

In the case of **4a**, there was one close contact between the carbonyl group of the quinozolinone core and Asn353A$^{6.55}$ (TM6). Compound **4a and 4b**, both showed π– bonding of quinozolinone core and Arg356A$^{6.58}$as seen in **L365, 260** and **YF476**. Compound **4a** also exhibited H-bond with residue Arg213 (EL2) and Vanderwaals interactions with Pro114A$^{2.64}$, Ala352A$^{6.54}$, Ile375A$^{7.38}$ and Thr111A$^{2.61}$ (Figure 3). The ligand **4a**also showed hydrophobic π– alkyl interactions with Arg356A$^{6.58}$, Val349A$^{6.51}$and Ala352A$^{6.54}$, whereas Leu113A$^{2.63}$, Pro114A$^{2.64}$ and Arg356A$^{6.58}$ were found to form π– alkyl hydrophobic bonds with **4b, as also reported in the case of 3c.** This is in agreement with reported interacting residues in earlier studies[29,30]. Similar to **YF476 and L365,260**, both **4a and 4b** were further stabilized by common van der Waals interactions to residues Pro114A$^{2.64}$, Ile375A$^{7.38}$and Val349A$^{6.51}$.

Therefore, the two amino acids Asn353A$^{6.55}$, Arg356A$^{6.58}$ (TM6), appear to be much more involved in antagonistic activity of all ligands through H-Bonds and several residues with hydrophobic interactions. The pharmacophore mapping results of **L365, 260** and **YF476** also exhibited four features namely two hydrogen bond donors and two hydrophobic features. These features/groups were found to be interacting within the binding site of the CCK-BR receptor through the similar groups in the ligands. Hence the ligand based approach used in our previous study[25] could be utilized here to optimize the compounds and docking of these compounds showed important binding interactions.

Biological Evaluation

Receptor Binding Assay and SAR

The affinity of the compounds for the CCK-BR was determined by a competitive binding assay with a Bolton-Hunter labelled CCK-8 radioligand, ^{125}I-BH-CCK-8 (Perkin Elmer). Compounds in both the series showed good binding activities in the range of 0.2 – 975 nM (Table 1). Compound **3c** with p-bromo substitution in ring A and m-COOH in ring B showed the highest affinity (IC_{50}0.200nM)followed by **3a**[23](p-OC_2H_5, ring A; m-COOH, ring B; IC_{50} 0.66 nM). Compound **3g** (p-OC_2H_5, ring A; p-Cl, ring B) showed IC_{50} 11.48 nM, whereas**3e** (p-Cl, ring A; p-OC_2H_5) and **3b** (m-Br, ring A; m-COOH, ring B) showed IC_{50} 9.715 and 8.64 nM respectively. Compound **3f (**p-OC_2H_5, ring A; p-Br, ring B) also showed good affinity (2.005 nM) whereas the unsubstituted ring A in compound **3d** resulted in IC_{50} 975 nM. Therefore, the substitution in Ring A is important for improving the activity and a polar substituent in ring B improves the activity.

The other series of compounds with hydrazino linker and substitution in only ring A and where ring B being indanone resulted in overall less active compounds. In this series the most active compound **4a** with p-OC_2H_5 substitution in ring A (IC_{50} 17.36 nM) favoured over p-CH_3 **(4b,** IC_{50} 56.49 nM). m-Br substitution in compound **4e** (IC_{50} 19.46 nM) in ring A resulted in better affinity over m-Cl (IC_{50} 384 nM),. Overall electron donating group improved the activity in this series of compounds.

To summarize the SAR, we suggest that overall the substitution in ring A is important for CCK-BR antagonistic activity with p-OC_2H_5 substitution (**3a**) and p-Br (**3c**) in Ring A along with m-COOH group in Ring Bbeing favourable in the series with hydrazinocarbothioamide linker. Both these compounds were also predicted highly active through pharmacophore mapping exercise and their actual activities correlated well to the estimated activities with fit values greater than 7 (designated as +++ in Table 1). The most favoured substitution in the compounds with hydrazino group as linker and indanone as Ring B was p-OC_2H_5 (**4a)** which was found to be active in *in vitro* binding experiment. Compounds **3c** and **4a** also exhibited favourable interactions in the CCK-BR binding site as discussed in docking results above and shown in Table 1.

Gastric acid secretion assay

To further establish the ability of the compounds in two series, these were tested to antagonize pentagastrin-induced gastric acid secretion in an isolated lumen perfused mouse stomach assay. All the compounds produced concentration dependent, non-parallel shifts to the right of the concentration response curves to Boc-pentagastrin[12,31] and decreased the maximum response. Therefore, pA2 (negative algorithm of the molar concentration of a dose of agonist to that of half the dose) could not be calculated. The compounds were capable of inhibiting the gastric acid secretion (Table 1) at 100 nM. The compounds showed almost 50-60 % inhibition and one compound with no substitution in ring A showed an inhibition of 39% at much higher concentration (1µM) again suggesting that the substitution in ring A is important for specific CCK-BR antagonistic activity in both the series of compounds.

Cytotoxicity Evaluation

All the compounds synthesized in this study were then tested for anti-proliferative activity against pancreatic cancer cells (MiaPaca-2) using MTT assay[32]. The growth inhibition effect evaluated through dose response graphs showed that all the quinazolinone derivatives exhibited growth inhibitory effect and IC_{50} in the range of 10 – 280 µM was obtained. The positive control for the experiment **L365, 260** showed IC_{50} of 0.0018 µM. The compound **3f**with hydrazine linker and substitution p-OC_2H_5 (Ring A) and p-Br (ring B) exhibited best IC_{50} (10 µM) whereas compound **4b** showed similar activity (IC_{50} 10 µM) in indole series. Therefore, our results provided two potent CCK-BR antagonists exhibiting good CCKBR antagonistic activity as well as cytotoxicity against CCK-BR expressing pancreatic cancer cells (MiaPaca-2) (Table 1).

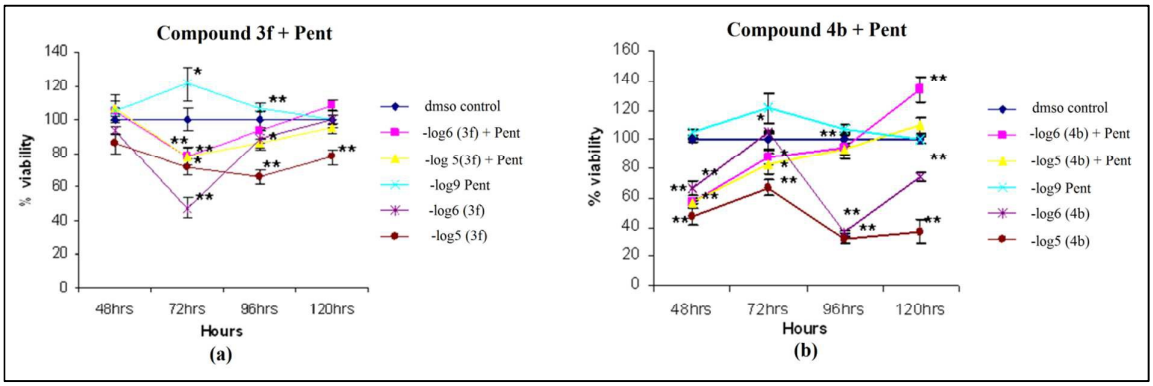

Figure 4: Time and concentration dependent effect of antagonist 3f and 4b on the cell viability of MIAPaCa 2 cells. The lines depict various concentrations of antagonists (alone), Boc-pentagastrin (alone) and/or antagonist and Boc-pentagastrin together. DMSO control at all the time points is taken as 100%.

Inhibition of proliferation of MiaPaca-2 cells induced by Boc-Pentagastrin

Smith et al [33] reported that the growth responses of several human pancreatic cancer cell lines are stimulated by CCK in serum-free medium, and its tropic effect can be blocked by a specific antagonist [5]. They also demonstrated that gastrin exerts a growth-stimulating effect on pancreatic cancer *in vivo* and *in vitro* [34]. Therefore, we checked whether the cytotoxicity shown by compounds **3f** and **4b** in MiaPaca-2 cells is specific towards gastrin induced proliferation or not. The cellular proliferation induced by one of the potent and specific CCK-BR agonist, Boc-Pentagastrin was undertaken. The Boc-Pentagastrin showed proliferative effect in the MiaPaca-2 cells from a concentration of 1 pM to 10µM tested for a time period of 48 h to 120 h. No cellular growth was observed in first 24 h. Maximum cellular growth was observed at 10nM at 96 h (also reported earlier)[33]. Both the compounds **3f** and **4b** were tested at 10µM (IC_{50} concentration as determined from MTT assay) and at 1 µM for evaluating their inhibitory effect on specific growth induced by Boc-Pentagastrin. The compounds exhibited anti-proliferative action against Miapaca-2 cells at both the tested concentrations (Figure 4a & 4b), exhibiting maximum inhibition at 72 h when given alone. The compounds also inhibited the proliferative effects of Boc-Pentagastrin when used in combination. Several studies have been performed to show presence of CCK-C receptor subtype in pancreatic cancers but not in normal tissues[35]. Our results suggest compounds **3f** and **4b** might show some kind of selectivity towards CCK-C receptors in MiaPaCa-2 cell line which has been shown to express this splice variant[9].

ADMET Prediction

The intestinal absorption and blood brain barrier penetration were predicted by developing an ADME model using descriptors 2D PSA and AlogP98 that include 95% and 99% confidence ellipses. These ellipses define regions where well-absorbed compounds are expected to be found. The results of DS 4.0-ADME model screening showed that both our active compounds **3f** and **4b** possess 99% confidence levels for human intestinal absorption, and low blood brain barrier (BBB) penetration. Since we are targeting pancreatic cancer, the low BBB penetration of our active compounds is advantageous.Also; TOPKAT results predicted that both **3f** and **4b** are non-toxic, non-mutagen and non-irritant to the skin, which makes our active compounds competitive to be new developmental compounds for the Pancreatic Cancer. Overall the compounds **3f** and **4b** are being suggested as the best compounds which showed good CCK-BR antagonistic activity, showed lower IC_{50} (cytotoxicity), specifically

View Article Online
DOI: 10.1039/C7MD00171A
ARTICLE Journal Name

inhibited the growth stimulatory effects of gastrin in MiaPaca-2 cells as well as exhibited best computed ADMET properties.

Experimental Section

Analytical grade materials were purchased from commercial suppliers and were used without purification, unless otherwise noted. Melting points were determined on a Thomas Hoover apparatus and are uncorrected. The ^{1}HNMR spectra were determined on a Bruker 300 MHz spectrometer at ambient temperature. IR spectroscopy was performed with a FTIR apparatus (Model 1600, Perkin Elmer). Mass spectra were recorded on AP1, PE SCEIX system. Fast atom bombardment (FAB) mass spectra were recorded with an SX 102/DA-6000 mass spectrometer (JEOL) with m-nitrobenzylalcohol as matrix, elemental analysis was done using a Carlo Erba 1108 (Heraus, Hanau, Germany). All experiments involving animals were approved by the Institutional Animal Ethics Committee under the Committee for the purpose of control and Supervision and Experimentation on Animals (CPCSEA), Ministry of Environment, Government of India.

General method for synthesis of 3-aryl-2-thioxo-2, 3-dihyroquinazolinone-4-(1*H*)-one (1a-f)
Anthralinic acid (3.0 g, 0.021 M) and appropriate substituted aryl isothiocynate(0.022 M) were refluxed in glacial acetic acid (75 mL) for 16 h. The white lustrous crystals was separated by filtration and washed with water until the washings showed neutral pH. The crystalline product was dried and checked for purity using TLC (ethyl acetate - petroleum ether in 50%).

3-(4-Methylphenyl)-2-thiooxo-2,3-dihydroquinazoline -4-(1*H*)-one (1a): Yield, 4.5 g (85 %);mp>300 ^{o}C; IR (KBr)ν_{max}/cm^{-1}; 3245.02 (NH), 1662.43 (C=O), 1200.05 (C=S); ^{1}H NMR (DMSO–d_6); δ 12.965 (Brs, 1H, D_2O exchangeable), 7.953(d, 1H, *J* = 7.8 Hz), 7.797 (t, 1H, *J* = 7.65 Hz), 7.450 (d, 1H, *J* = 8.1 Hz), 7.359 (t, 1H, *J* = 6.0 Hz), 7.276 (d, 2H, *J* = 6.6 Hz), 7.140 – 7.120 (m, 1H), 2.364 (S, 3H).

3-(4-ethoxyphenyl)-2-thiooxo-2,3-dihydroquinazoline-4-(1*H*)-one (1b): Yield, 4.914g (80%);mp 285 ^{o}C;IR (KBr)ν_{max}/cm^{-1}; 3223.54(NH), 1662.59 (C=O), 1205.10 (C=S). ^{1}H NMR (DMSO–d_6);δ 11.987 (Brs., 1H, D_2O exchangeable), 7.942 (d,1H, *J* = 8.7 Hz), 7.688–7.637 (m, 2H), 7.339 (t, 1H, *J* = 5 Hz), 7.122 (d, 2H, *J* = 8.7 Hz), 6.809 (d, 2H, *J* = 9.0 Hz), 4.223 (q, 2H, *J* = 6.8 Hz), 1.392 (t, 3H, *J* = 6.9 Hz).

3-phenyl-2-thiooxo-2,3-dihydroquinazoline-4-(1*H*)-one (1c): Yield, 1.930 g (90 %);mp>300°C, IR (KBr)ν_{max}/cm^{-1}; 3219 (NH), 1662.5 (C=O), 1197.7 (C=S), ^{1}H NMR (DMSO–d_6);δ13.037 (Brs, 1H, D_2O exchangeable), 7.958 (d, 2H, *J* = 7.8 Hz), 7.798 (t, 2H, *J* = 5.0 Hz), 7.472–7.253 (m, 5H).

3-(4-bromophenyl)-2-thiooxo-2,3-dihydroquinazoline-4-(1*H*)-one (1d): Yield, 1.608 g (99%);mp>320°C; IR (KBr)ν_{max}/cm^{-1};3235.35 (NH),1663 (C=O),1199.05 (C=S), ^{1}H NMR (DMSO–d_6);δ13.097 (Brs, 1H, D_2O exchangeable), 7.973 (d, 1H, *J* = 7.8 Hz), 7.839 (t, 1H, *J* = 5.1 Hz), 7.695 (d, 2H, *J* = 7.2 Hz), 7.461 (d, 1H, *J* = 8.1 Hz), 7.383 (t, 1H, *J* = 5.0 Hz) 7.290 (d, 2H, *J* = 7.2 Hz).

3-(4-chlorophenyl)-2-thiooxo-2,3-dihydroquinazoline-4-(1*H*)-one (1e): Yield, 1.783 g (100%);mp>320°C; IR (KBr)ν_{max}/cm^{-1};3246.0 (NH), 1662.5 (C=O), 1199.6 (C=S), 759.9 (C-Cl), ^{1}H NMR (DMSO–d_6);δ 11.971 (Brs, 1H, D_2O exchangeable), 7.964 (d, 1H, *J* = 6.3 Hz) 7.815 (t, 1H, *J* = 7.6 Hz), 7.557 (d, 1H, *J* = 5.0 Hz), 7.445–7.376 (m, 4H), 7.350–7.267 (m, 1H).

3-(3-chlorophenyl)-2-thiooxo-2,3-dihydroquinazoline-4-(1*H*)-one (1f): Yield, 1.67 g (98%);mp298 °C; IR (KBr)ν_{max}/cm^{-1};3205 (NH), 1664.78 (C=O), 1199.21(C=S), 761 (C-Cl), ^{1}H NMR (DMSO–d_6);δ13.105 (Brs, 1H, D_2O exchangeable), 7.974 (d, 1H,*J* = 7.2 Hz), 7.824 (t, 1H, *J* = 7.6 Hz), 7.548 – 7 .468 (m, 3H), 7.439 (s, 1H), 7.388 (d, 1H, *J* = 7.5 Hz)7.338 (t, 1H, *J* = 7.0 Hz).

3-(3-bromophenyl)-2-thiooxo-2,3-dihydroquinazoline-4-(1*H*)-one (1g): Yield: 0.50 g (38%); mp295 °C, IR (KBr)ν_{max}/cm^{-1};3210 (NH), 1672.42 (C=O), 1197.74 (C=S), ^{1}H NMR(DMSO–d_6); δ13.105 (Brs, 1H, D_2O exchangeable), 7.973 (d, 1H, *J* = 8.1 Hz), 7.824 (t, 1H, *J* = 7.6 Hz), 7.636–7.612 (m, 2H), 7.462 (d, 2H, *J* = 7.5 Hz), 7.386–7.334 (m, 2H).

General procedure for synthesis of 2-hydrazino-3-arylquinazoline-4-(3H)-one (2a-g)

View Article Online
DOI: 10.1039/C7MD00171A

A mixture of 1(0.016 M) and anhydrous hydrazine (5.87 mL, 0.16 M) in anhydrous methanol was refluxed for 18 h. The solid was separated by filtration, washed with cold methanol and was dried.

2-hydrazino-3-(4-methylphenyl)quinazoline -4-(3H)-one (2a): Yield, 2.2 g (71%);mp 193–194 °C; IR (KBr)ν_{max}/cm^{-1}; 3497.67, 3311.65, 3209.05 (NH's), 1673.02 (C=O); ^{1}H NMR (DMSO–d_6);δ7.925 (d, 1H, *J* = 7.8 Hz), 7.787–7.761 (d, 1H, *J* = 7.8 Hz), 7.670 (t, 1H, *J* = 7.0 Hz), 7.389(m, 1H), 7.361 (d, 2H, *J* = 7.5 Hz), 7.187 (d, 2H, *J* = 7.8 Hz), 6.787 (Brs, 1H, D_2O exchangeable), 4.391 (Brs, 2H, D_2O exchangeable), 2.393 (s, 3H).

2-hydrazino-3-(4-ethoxyphenyl)quinazoline-4-(3H)-one (2b): Yield, 3.4 g (79 %);mp 222 °C;IR (KBr)ν_{max}/cm^{-1}; 3423.4 (NH-NH_2), 1706.9 (C=O), ^{1}H NMR (DMSO–d_6);δ7.924 (d, 1H, *J* = 7.8 Hz), 7.669 (t, 1H, *J* = 7.6 Hz), 7.359 (d, 1H, *J* = 7.2 Hz), 7.211 (d, 2H, *J* = 8.7 Hz), 7.158 (t, 1H, *J* = 5.0 Hz), 7.070 (d, 2H, *J* = 9.0 Hz), 6.906 (Brs, 1H, D2O, exchangeable), 4.458 (Brs,2H, D2O exchangeable), 4.122–4.053 (q, 2H, *J* = 6.9 Hz), 1.392–1.346 (t, 3H, *J* = 6.9 Hz).

2-hydrazino-3-phenylquinazoline-4-(3H)-one (2c): Yield, 2.5 g (80 %);mp 205 °C;IR (KBr)ν_{max}/cm^{-1}; 3487.67, 3229.05 (NH's), 1673.02 (C=O), ^{1}H NMR (DMSO–d_6);δ 8.220 (Brs, 1H, D_2O exchangeable),7.910 (m, 2H), 7.655 (d, 1H, *J* = 7.2 Hz), 7.557 (m, 2H, *J* = 8.4 Hz), 7.399 (d, 1H, *J* = 8.1 Hz), 7.372–7.327 (m, 2H), 7.161 (d, 1H, *J* = 7.8 Hz), 4.419 (Brs, 2H, D_2O exchangeable).

2-hydrazino-3-(4-bromophenyl)quinazoline-4-(3H)-one (2d): Yield, 0.185 g (37%); mp 210 °C; IR (KBr)ν_{max}/cm^{-1};3291.67, 3330.86 (NHs), 1676.23 (C=O), ^{1}H NMR (DMSO–d_6); δ8.225 (Brs, 1H, D_2O exchangeable), 8.011 (d, 1H, *J* = 7.8 Hz), 7.962 (d, 2H, *J* = 8.1 Hz), 7.694 (t, 1H, *J* = 7.5 Hz), 7.543 (d, 2H, *J* = 8.4 Hz), 7.413 (d, 1H, *J* = 8.1 Hz), 7.278 (t, 1H, *J* = 7.5 Hz), 4.386 (Brs, 2H, D_2O exchangeable).

2-hydrazino-3-(4-chlorophenyl)quinazoline-4-(3H)-one (2e): Yield, 0.58 g (58%);mp 190 °C; IR (KBr)ν_{max}/cm^{-1};3210.33, 3306.27 and 3328.41 (NHs), 1675.57 (C=O), ^{1}H NMR (DMSO–d_6); δ8.352 (Brs, 1H, D_2O exchangeable), 8.022 (d, 1H, *J* = 9.9 Hz), 7.940 (d, 1H, *J* = 9.0 Hz), 7.693 (t, 1H, *J* = 7.5 Hz), 7.422 (d, 2H, *J* = 9.0 Hz), 7.331 (d, 2H, *J* = 8.4 Hz), 7.251 (t, 1H, *J* = 7.5 Hz), 4.41 (Brs, 2H, D_2O exchangeable).

2-hydrazino-3-(3-chlorophenyl)quinazoline-4-(3H)-one (2f)*:* Yield, 0.267 g (26%), mp 170 °C; IR (KBr)ν_{max}/cm^{-1};3312.35 (NHs) 1674.79 (C=O), 759.19 (C-Cl), ^{1}H NMR (DMSO–d_6);δ8.823 (Brs, 1H, D_2O exchangeable), 8.025 (d, 1H, *J* = 7.8 Hz), 7.290 (d, 1H, , *J* = 5.0 Hz), 7.131 (d, 1H, *J* = 7.8 Hz), 7.404 (d, 1H, *J* = 8.1 Hz), 7.686 (t, 1H, *J* = 4.0 Hz), 7.574 - 7.493 (m, 2H), 4.370 (Brs, 2H, D_2O exchangeable).

2-hydrazino-3-(3-bromophenyl)quinazoline-4-(3H)-one (2g): Yield, 0.289 g (28%);mp 190°C; IR (KBr)ν_{max}/cm^{-1};3306.60 (NHs), 1672.42 (C=O), ^{1}H NMR(DMSO–d_6); δ8.248 (Brs, 1H, D_2O exchangeable), 4.382 (Brs, 2H, D_2O exchangeable), 8.025(d, 1H, *J*= 7.8 Hz), 7.971 (d, 1H, *J* = 7.8 Hz), 7.822 (t, 1H, *J* = 7.6 Hz), 7.711–7.661 (t, 1H,, *J* = 7.5 Hz), 7.61 (s, 1H), 7.461–7.266 (m, 3H).

General method for synthesis of {N-aryl-2-[3,4-dihydro-3 or 4-substituted aryl)-4-oxo-2 quinazonyl]}hydrazine carbothioamide (3a-g)

An equimolar mixture of appropriate compound 2 (0.878 mM) and 3- or 4-substituted arylisothiocynate (0.878 mM) was stirred in DMF under inert atmosphere at 110 ºC for 12 h. DMF was evaporated by using rotavapour. The residue obtained was washed with cold methanol, filtered and dried to give **3a-g**.

3-(2-(3-(4-ethoxyphenyl)-4-oxo-3,4-dihydroquinazolin-2-yl)hydrazinecarbothioamido)benzoic acid(3a): Yield, 1.90 g (60 %); mp 239 °C;IR (KBr)ν_{max}/cm^{-1}; 3442.5 (NH), 1662.5 (C=O), 1249.8 (C=S), 2924.52 (-OC_2H_5); ^{1}H NMR (DMSO–d_6);δ 12.995 (s, 1H, D_2O exchangeable), 11.500 (Brs, 1H, D_2O exchangeable), 9.520 (Brs, 1H, D_2O exchangeable), 8.234 (Brs, 1H, D_2O exchangeable), 8.207 (s, 1H), 7.955 (d,*J*= 7.56, 1H), 7.796 (t, 1H,*J* = 7.6 Hz), 7.686 (t, 1H, *J* = 7.5 Hz), 7.446 (d, 1H, *J* = 8.34 Hz), 7.381 (t, 1H, *J* = 7.652 Hz), 7.204 – 7.314 (m, 1H), 7.204(d, 2H, , *J* = 8.1 Hz), 7.094 (d, 1H, *J* = 7.8 Hz), 6.994 (d, 2H,

View Article Online
DOI: 10.1039/C7MD00171A
ARTICLE Journal Name

J= 7.9 Hz), 4.101(q, 2H, , *J* = 6.4 Hz), 1.380 (t, 3H, , *J* = 6.6 Hz); MASS (*m/z)* = 474 ($C_{24}H_{21}N_5SO_4$[M – 1]$^+$).Anal.Calcd.for $C_{24}H_{21}N_5SO_4$: C, 60.62; H, 4.45; N, 14.73.Found:C, 60.76; H, 4.52; N, 14.89.

3-(2-(3-(3-bromophenyl)-4-oxo-3,4-dihydroquinazolin-2-yl)hydrazinecarbothioamido)benzoic acid(3b): Yield: 0.658 g (65 %);mp 195 °C;IR (KBr)ν_{max}/cm^{-1}; 3327.92 (NH), 1670.16 (C=O), 1197.92 (C=S), 759.96 (C-Br); ^{1}H NMR (DMSO–d_6);δ12.564 (s, 1H, D_2O exchangeable), 11.545 (Brs, 1H, D_2O exchangeable), 9.296 (Brs, 1H, D_2O exchangeable), 8.503 (Brs, 1H, D_2O exchangeable), 8.384 (d, 1H, *J* = 7.6 Hz), 7.976 (d, 1H, *J* = 8.3 Hz), 7.984 (t, 1H, *J* = 5.0 Hz), 7.892 (d, 1H, *J* = 7.2 Hz), 7.836 - 7.829 (m, 3H), 7.908 (d, 2H, *J* = 7.8 Hz), 7.743 - 7.712 (m, 1H), 6.923 (d, 2H, *J* = 5.0 Hz); MASS (*m/z*) M$^+$= 509 ($C_{22}H_{16}BrN_5O_3S$).Anal.Calcd.for$C_{22}H_{16}BrN_5O_3S$:C, 51.77; H, 3.16; N, 13.72. Found: C, 51.89; H, 3.28; N, 13.83.

3-(2-(3-(4-bromophenyl)-4-oxo-3,4-dihydroquinazolin-2-yl)hydrazinecarbothioamido)benzoic acid (3c): Yield, 0.352 g (50 %);mp220 °C;IR (KBr)ν_{max}/cm^{-1}; 3330.73 (NH), 1676.02 (C=O), 1223.82 (C=S), 762.19 (C-Br), ^{1}H NMR (DMSO–d_6);δ12.539 (s, 1H, D_2O exchangeable), 11.691 (Brs, 1H, D_2O exchangeable), 9.295 (Brs, 1H, D_2O exchangeable), 8.399 (Brs, 1H, D_2O exchangeable), 8.359 (d, 1H, *J* = 6.3 Hz), 7.975 (d, 1H, *J* = 9.4 Hz), 7.940 (t, 1H, *J* = 7.2 Hz), 7.892 (d, 1H, *J* = 7.3 Hz), 7.836 – 7.819 (m, 3H), 7.808 (d, 2H, *J* = 7.8 Hz), 7.753 – 7.712 (m, 1H), 6.823 (d, 2H, *J* = 5.1 Hz);MASS(m/z) M+ = 509($C_{22}H_{16}BrN_5O_3S$).Anal.Calcd.for$C_{22}H_{16}BrN_5O_3S$: C, 51.77; H, 3.16; N, 13.72. Found: C, 51.88; H, 3.29; N, 13.85.

3-(2-(4-oxo-3-phenyl-3,4-dihydroquinazolin-2-yl)hydrazinecarbothioamido)benzoicacid(3d): Yield, 1.354 g (50 %);mp263 °C; IR (KBr)ν_{max}/cm^{-1}; 3435.92 (NH), 1675.93 (C=O), 1298.66 (C=O); ^{1}H NMR (DMSO–d_6);δ12.784 (s, 1H, D_2O exchangeable), 11.504 (Brs, 1H, D_2O exchangeable), 9.534 (Brs, 1H, D_2O exchangeable), 8.292 (Brs, 1H, D_2O exchangeable), 8.334 (d, 1H, *J* = 7.8 Hz), 7.956 (d, 1H, *J* = 9.4 Hz), 7.924 -7.909 (t, 1H, *J* = 5.0 Hz), 7.892 (d, 1H, *J* = 7.2 Hz), 7.836 - 7.829 (m, 3H), 7.908 (d, 2H, *J* = 9.2 Hz), 7.743 - 7.712 (m, 2H), 6.723 (d, 2H, *J* = 5.0 Hz);MASS (*m/z*) M$^+$ = 431 ($C_{22}H_{17}N_5O_3S$).Anal.Calcd.for$C_{22}H_{17}N_5O_3S$:C, 61.24; H, 3.97; N, 16.23. Found: C, 61.39; H, 3.90; N, 16.10.

N-(4-chlorophenyl)-2-(3-(4-ethoxyphenyl)-4-oxo-3,4-dihydroquinazolin-2-yl)hydrazinecarbothioamide (3e): Yield, 0.798 g (65 %);mp242 – 244 °C; IR (KBr)ν_{max}/cm^{-1}; 3330 (NH), 1698.94 (C=O), 1296.55 (C=S), 2967.2 (C-H); ^{1}H NMR (DMSO–d_6); δ10.775 (Brs, 1H, D_2O exchangeable), 9.932 (Brs, 1H, D_2O exchangeable), 8.659 (Brs, 1H, D_2O exchangeable), 7.955 (d, 1H, *J* = 7.2 Hz), 7.797 (t, 1H, *J* = 7.6 Hz), 7.544(t, 1H, *J* = 9.3 Hz), 7.450 (d, 1H, *J* = 8.7 Hz), 7.395 (d, 2H, *J* = 9.0 Hz), 7.164 (d, 2H, *J* = 8.7 Hz), 7.078 (d, 2H, *J* = 8.7 Hz), 6.994 (d, 2H, *J* = 8.7 Hz), 4.131 (q, 2H, *J* = 7.0 Hz), 1.391 (t, 3H, *J* = 6.8 Hz).MASS (*m/z*) M$^+$= 465 ($C_{23}H_{20}ClN_5O_2S$).Anal.calcd. for$C_{23}H_{20}ClN_5O_2S$: C, 59.29; H, 4.33; N, 15.03. Found: C, 59.10; H, 4.25; N, 15.21.

N-(4-bromophenyl)-2-(3-(4-ethoxyphenyl)-4-oxo-3,4-dihydroquinazolin-2-yl)hydrazinecarbothioamide (3f): Yield, 0.285 g (57 %); mp>250°C;I.R.(KBr) ν_{max}/cm^{-1}; 3400 (NH), 1662.83 (C=O), 1250.86(C=S), 2967.06 (C-H); ^{1}H NMR, (DMSO–d_6);δ 10.945 (Brs, 1H, D_2O exchangeable), 10.235 (Brs, 1H, D_2O exchangeable), 9.198 (Brs, 1H, D_2O exchangeable), 8.246 (d, 1H, *J* = 6.6 Hz), 7.918 (d, 2H, *J* = 7.8 Hz), 7.699 (d, 2H, *J* = 7.5 Hz), 7.363 - 7.298 (m, 4H), 7.198 (d, 1H, *J* = 7.2 Hz), 6.860 (d, 2H, *J*= 7.5 Hz), 3.992 (q, 2H, *J* = 6.2 Hz), 1.342 (t, 3H, *J* = 6.1 Hz); MASS (*m/z*) M$^+$= 509 ($C_{23}H_{20}BrN_5O_2S$).Anal.calcd. for$C_{23}H_{20}BrN_5O_2S$: C, 54.12; H, 3.95; N, 13.72. Found: C, 54.28; H, 3.86; N, 13.91.

2-(3-(4-chlorophenyl)-4-oxo-3,4-dihydroquinazolin-2-yl)-N-(4-ethoxyphenyl)hydrazinecarbothioamide (3g): Yield, 0.82 g (72 %); mp 260 °C; IR (KBr)ν_{max}/cm^{-1}; 3435.26 (NH), 1616.47 (C=O), 1225.79 (C=S), 2973.73 (C-H); ^{1}H NMR (DMSO–d_6); δ13.355 (Brs, 1H, D_2O exchangeable), 10.450 (Brs, 1H, D_2O exchangeable), 10.303 Brs, 1H, D_2O exchangeable), 8.123 (d, 1H, *J* = 8.1 Hz), 7.990–7.921 (m, 1H), 7.831 (d, 1H, *J* = 7.8 Hz), 7.588 (d, 2H, *J* = 7.6 Hz), 7.399–7.324 (m, 4H), 7.270 (t, 1H, *J* = 7.5 Hz), 7.106 (d, 2H,*J* = 8.4 Hz), 4.116 (q, 2H, , *J* = 6.6 Hz), 1.388 (t, 3H, *J* = 6.4 Hz); MASS (m/e) M$^+$= 465 ($C_{23}H_{20}ClN_5O_2S$). Anal.calcd. for$C_{23}H_{20}BrN_5O_2S$: C, 59.29; H, 4.33; N, 15.03. Found: C, 59.12; H, 4.40; N, 15.18.

General procedure for synthesis of (Z)-3-aryl-2-(2-(2-oxoindolin-3-ylidene)hydrazinyl)quinazolin-4(3H)-one(4a-e)

View Article Online
DOI: 10.1039/C7MD00171A

An equimolar mixture of 2, 3-dioxoindole (0.499 g, 0.0034 M) and appropriate 2-hydrazino-3-arylquinazoline- 4(3H)-one (0.0034 M) was refluxed in 50 mL of absolute ethanol for 2 h. The precipitate thus formed was filtered, washed with cold ethanol, dried and crystallized from ethanol to give the compounds **4a-e**.

(Z)-3-(4-ethoxyphenyl)-2-(2-(2-oxoindolin-3-ylidene)hydrazinyl)quinazolin-4(3H)-one (4a): Yield, 2.5 g (90%); mp 275 - 280 °C;IR (KBr)ν_{max}/cm^{-1}; 3064.7, 3184.3 (NH's), 1708.8 and 1622 (C=O); ^{1}H NMR (DMSO–d$_6$); δ11.51 (s, 1H, D$_2$O exchangeable), 10.4696 (S, 1H, D$_2$O exchangeable), 8.006 (d, 1H, *J* = 7.5 Hz), 7.856 (d, 1H, *J* = 8.4 Hz), 7.767 (t, 1H, *J* = 7.2 Hz), 7.340 (d, 2H, *J* = 8.7 Hz), 7.311 (t, 1H, *J* =8.6 Hz), 7.176 (t, 1H, *J* = 7.2 Hz), 7.128 (d, 2H, *J* = 8.7 Hz), 6.980 (d, 1H, *J* = 7.5 Hz), 6.755 (d, 1H, *J* = 7.5 Hz), 6.520 (t, 1H, *J* = 7.5 Hz), 4.112–4.06 (q, 2H, *J* = 6.8 Hz), 1.380 (t, 3H, *J* = 6.6 Hz); MASS (*m/z*)M$^+$ = 425 ($C_{24}H_{19}N_5O_3$). Anal.calcd. for$C_{24}H_{19}N_5O_3$: C, 67.76; H, 4.50; N, 16.46. Found: C, 67.51; H, 4.62; N, 16.30.

(3Z)-1H-indole-2,3-dione 3-{[3- (4-methylphenyl)-4-oxo-3,4-dihydroquinazolin-2- yl]hydrazone} (4b): Yield, 0.6 g (68%);mp 280 °C;IR (KBr)ν_{max}/cm^{-1}; 3184.2 (NH), 1708.7 (C=O);^{1}H NMR (DMSO–d$_6$); δ11.53 (Brs, 1H, D$_2$O exchangeable), 10.43 (s, 1H, D$_2$O exchangeable), 8. (d, 1H, *J* = 7.5 Hz), 7.879 (d, 1H, *J* = 9.2 Hz), 7.768 (t, 1H, *J*=6.6 Hz Hz), 7.407 (d, 2H, *J* = 8.1 Hz), 7.310 (t, 2H, *J* = 8.2 Hz), 7.154 (t, 2H, *J* =6.2 Hz), 6.839 (d, 1H, *J* = 7.5 Hz), 6.740 (d, 1H, *J* = 7.5 Hz), 6.501 – 6.451 (t, 1H, *J* =7.47 Hz), 2.45 (s, 3H). MASS (*m/z*) M$^+$ = 395 ($C_{23}H_{17}N_5O_2$).Anal.calcd. for: C, 69.86; H, 4.33; N, 17.71. Found:C, 69.69; H, 4.44; N, 17.57.

(3Z)-1H-indole-2,3-dione-3-{[4- (4-chlorophenyl)-4-oxo-3,4-dihydroquinazolin-2- yl]hydrazone} (4c): Yield, 0.269 g (70%); mp 280 °C; IR (KBr)ν_{max}/cm^{-1}; 3313.58 (NH's), 1691.14 (C=O);^{1}H NMR (DMSO–d$_6$); δ11.632 (Brs, 1H, D$_2$O exchangeable), 10.622 (Brs, 1H, D$_2$O exchangeable), 8.455 (d, 1H, *J* = 8.4 Hz), 8.027 (d, 1H, *J* = 7.5 Hz), 7.818 (d, 2H, *J* = 8.7 Hz), 7.739 – 7.641 (m, 1H), 7.421 – 7.291 (m, 4H), 7.061 (t, 2H, *J* = 7.5 Hz), 6.896 (d, 1H, *J* = 7.8 Hz); MASS (*m/z*) M$^+$ = 415 ($C_{22}H_{14}ClN_5O_2$).Anal.calcd. for$C_{22}H_{14}ClN_5O_2$: C, 63.54; H, 3.39; N, 16.84. Found: C, 63.39; H, 3.48; N, 16.70.

(3Z)-1H-indole-2,3-dione 3-{[3- (3-chlorophenyl)-4-oxo-3,4-dihydroquinazolin-2- yl]hydrazone} (4d): Yield, 0.052 g (34%);mp 335 °C; IR (KBr)ν_{max}/cm^{-1}; 3434.84 (NH), 1623.32(C=O), 756.94 (C-Cl);^{1}H NMR (DMSO–d$_6$); δ11.70 (Brs, 1H, D$_2$O exchangeable), 10.58 (Brs, 1H, D$_2$O exchangeable), 8.018 (d, 1H, *J* = 8.1 Hz), 6.91 (d, 1H, *J* = 6.9 Hz), 6.777 (d, 1H, *J* = 7.8 Hz), 6.600 (t, 1H, *J* = 6.6 Hz), 7.322 (t, 1H, *J* = 8.1 Hz), 7.188 (t, 1H, *J* = 8.2 Hz), 7.810 - 7.762 (m, 3H), 7.677 - 7.641 (m, 3H); MASS (*m/z*) M$^+$ = 415 ($C_{22}H_{14}ClN_5O_2$).Anal.calcd. for$C_{22}H_{14}ClN_5O_2$: C, 57.41; H, 3.07; N, 15.22. Found: C, 57.27; H, 3.22; N, 15.39.

(3Z)-1H-indole-2,3-dione 3-{[3- (3-bromophenyl)-4-oxo-3,4-dihydroquinazolin-2- yl]hydrazone} (4e): Yield, 0.050 g (38%);mp295 °C; IR (KBr)ν_{max}/cm^{-1}; 3332.73(NH), 1710.51(C=O);^{1}H NMR (DMSO–d$_6$); δ13.141 (Brs, 1H, D$_2$O exchangeable), 11.644 (Brs, 1H, D$_2$O exchangeable), 8.012 – 7.943 (m, 1H), 7.876 (d, 1H, *J* = 8.4 Hz), 7.805 – 7.758 (m, 2H), 7.609 – 7.433 (m, 2H), 7.385 – 7.266 (m, 2H), 7.236 (t, 1H, *J* = 7.5 Hz), 6.907 (d, 1H, *J* = 7.5), 6.769 (d, 1H, *J* = 7.5 Hz) 6.612 (t, 1H, *J* = 7.5 Hz); MASS (m/e) M$^+$ = 459 ($C_{22}H_{14}BrN_5O_2$). Anal.Calcd.for$C_{22}H_{14}BrN_5O_2$: C, 63.54; H, 3.39; N, 16.84. Found: C, 63.36; H, 3.29; N, 16.98.

Molecular modeling

All molecular modeling work was performed using Discovery Studio 2.5.5 and Discovery Studio 4.0 (Accelrys Inc.). The molecules were built using "Builder" module. The energies were minimized using "CHARMm" force field in a step wise manner by using "steepest descent" followed by "conjugate gradient" till a RMSD derivative of 0.001 was achieved. Conformational models of the molecules were generated using "best quality" conformational search option in "Catalyst" using a constraint of 20 kcalmol^{-1} energy threshold above the global energy minimum and "CHARMm" force field parameters. A maximum of 250 conformations were generated using "best fit method" to ensure maximum coverage in the conformational space. The pharmacophore mapping exercise was performed using "Best mapping" protocol keeping the "flexible method" and "maximum omitted features" at 2. All the activities were predicted as nM and fit values were calculated by the software.

View Article Online
DOI: 10.1039/C7MD00171A
ARTICLE
Journal Name

Homology Modeling

The sequence of Human CCK-BR (ID: P32239), was retrieved from SwissProt database[36].The template structure and sequence of Human A2A Adenosine Receptor X-ray structure (3EML)[37] were downloaded from PDB (www.rcsb.org).The sequence alignment was generated with Clustal W multiple sequence alignment tool and manually adjusted to avoid insertions and deletions in the transmembrane regions.

The intracellular loop (IL3) of CCKBR was deleted as the template 3EML lacked this region. Most of the third cytoplasmic loop (Leu $209^{5.70}$ – $Ala221^{6.23}$ of the template was replaced with lysozyme from T4 bacteriophage and the carboxyl terminal tail (Ala317-Ser412) was deleted in the template 3EML.pdb to improve the likelihood of crystallization. Moreover, it has also been reported that most of the ligands binds to the extracellular region and the conserved transmembrane region of the CCK-BR[38]. Hence coordinates for this region could not be generated for this study.

Total 10 models of the CCK-BR along with 30 loop models were built using "MODELER" module present in Discovery Studio 4.0 at low optimization level. The loop modeling was performed for the modeling of gaps created during the sequence alignment. For the specific case of CCK-BR, the conserved disulphide bridge between Cys127 and Cys205 was manually introduced according to experimental data[39]. This disulphide bridge has importance in ligand binding interaction and the structure stability of the protein. All the models were sorted on the basis of their PDF total energy as well as DOPE score. A model is better optimized against the homology restraint when it has a lower PDF total energy.

For accessing the validity of homology model with sequence of residues it contain, verify score of each model was calculated by using "Profile-3D" module present in the Discovery studio 4.0. Finally the model having lowest PDF total energy score as well as highest verify score was selected for molecular dynamics simulations

Molecular Dynamics Simulation

The modelled structure of the CCK-BR generated above was used as starting structure for molecular dynamics simulations. The stability of the structure was verified through the molecular dynamics (MD) simulations using GROMACS[40] in an explicit membrane aqueous system. The total system consisted of 123 molecules of DPPC lipids, 31444 water molecules, 358 amino acids, Na^+ and Cl^- ions. Energy minimization was carried out by steepest descent algorithms applying Berger lipids parameters[41] for the lipid component in combination with the GROMOS[42] representation of the protein. Energy minimization was carried out by steepest descent algorithm with strong position restrained force on protein, so that, the protein position does not change during energy minimization. The steepest descent algorithm converged to F_{max}<1000 KJ/mol/nm in 1248 steps. Parinello- Rahman coupling[43], Berendson[44] and Nose- Hoover thermostat coupling[45] were used to equilibrate the system in stable environment (323K, 1bar). Electrostatic energy was computed by Particle Mesh Edwald (PME) method[46] and linear constraint solver (LINCS) algorithm[47] was applied to fix all bonds involving hydrogen. The structure in the medium was equilibrated for 100ps in NVT followed by 1000 ps in NPT due to membrane simulation. Finally, a 4 nanosecond molecular dynamics simulation was carried out for the structure.The RMSD (root-mean-square deviations) from the initial structure was calculated during 4ns simulation run. After MD simulation, the stereochemistry quality of the structures was validated with PROCHECK[48] and Verify 3D[49] and the quality factors of the protein models were calculated using ERRAT2[50], available in SAVES (Structural Analysis and Verification Server) [http://nihserver.mbi.ucla.edu/SAVES/]. The Ramachandran plot[51] was created by submitting the model toPDBsum[52].

Molecular Docking

All molecular docking work was done using Discovery Studio 4.0 software packages (Accelrys, California, USA). All the simulations were performed on Intel(R) Pentium(R) IV 2.4GHz, running Windows XP professional version 2006 operating system. The modelled structure was defined as the receptor molecule and was chosen for 'input receptor molecule parameter in the C-DOCKER protocol for molecular docking.All the molecules **YF476, L365,260,**

View Article Online
DOI: 10.1039/C7MD00171A
Journal Name ARTICLE

the synthesized compounds **3a-g** and **4a-e** were drawn and energy minimized in separate molecular windows and saved as *.dsv*file. The saved structures were then used as 'input ligands' in CDOCKER protocol and docked into the active site of CCK-BR.

ADME parameters screening for drug likeness

The compounds were subjected to ADMET calculations. Parameters such as aqueous solubility, absorption, plasma protein binding, cytochrome P450 2D6 inhibition, and hepatotoxicity were determined using the ADMET protocol in DS4.0 (Table TS1 and Figure S6 in supplementary file). Moreover, the toxicity potential (i.e., carcinogenicity and mutagenicity) of the compounds was also predicted using the TOPKAT (TOxicity Prediction by Komputer Assisted Technology) protocol in DS4.0 (Table TS2 in supplementary file).

Biological evaluation

Receptor binding assay

The affinity of the test compounds for the CCK-B/gastrin receptor, solubilized in detergent, was determined by a competitive binding assay with a Bolton–Hunter-labelled CCK-8 radioligandas previously described[53]. For this plasma membrane prepared from rat cerebral cortex (100 µg per tube) was mixed with ^{125}I-Bolton Hunter-CCK-8 (Perkin Elmer) radio-ligand (20 pM) in absence and presence of increasing concentrations of the test compounds. Non-specific binding was determined in presence of 1 µM unlabeled **CCK-8s** peptide (Bachem, Bubendorf, Switzerland). The tubes were incubated at 25 °C for 1 h to achieve steady state binding. Bound radio-ligand was rapidly separated from free radio-ligand using Millipore receptor binding filtermats. Bound radioactivity was quantified with Microbeta liquid scintillation counter from Perkin Elmer. Data was analysed using Graphpad software using non-linear least square curve fitting routine in the prism 5 software of the program.

Gastric acid secretion inhibition assay

For determination of acid secretion, the whole stomach was excised from albino mice (25-30 g) and was placed in tissue organ bath purchased from local suppliers and perfused by the methods described by Black et. Al[54]. The effluent from the perfused stomach was monitored for change in pH using continuous probe (Ecoscan pH meter from Eutech Instruments) inserted into the organ bath. The basal acidic pH and increase in acid output was produced by a sub-maximal concentration of Boc-pentagastrin (10 nM) before and 45 min after incubation with various concentrations of the test compound and the resultant percentage inhibition was calculated.

In vitro cytotoxicity assay

Cell survival was measured by using the MTT[3-(4, 5-dimethylthiazol-2-yl)-2, 5- diphenyltetrazolium bromide] micro-culture tetrazolium assay, according to the method described by Mosmann[32]. A total of 1000 cells/well were seeded in a 96-well plate. After 24 h incubation in a 5% humidified CO_2 incubator at 37°C, varying concentrations of compounds were added to final volume of 200 µL of standard growth medium/well. After 24 h incubation at 37°C, 20 µl of MTT (Invitrogen) (5 mg/mL in PBS) was added to each well and incubated for 4 h at 37°C. The medium was removed and formazancrystals thus formed were dissolved in DMSO. The plates were read immediately in a microplate reader (Tecan, GENios-Pro, Austria) operating at 540 nm.

Exogenous Gastrin Assay

The tropic effects of gastrin to promote tumour growth can be blocked by specific antagonists[33]. To show whether the stimulatory effect of gastrin was blocked by **3f** and **4b**, the MiaPaca-2 cells were incubated with Boc-Pentagastrin (Bachem)

View Article Online
DOI: 10.1039/C7MD00171A
ARTICLE Journal Name

for 24 h and then treated with **3f**, **4b** and Boc-pentagastrin either alone or in combination. Cellular proliferation was studied using the MTT assay as described above. Briefly, the cells were seeded in 96 well plate (4000cells/well) in 10% FCS-DMEM. Cells were then incubated in incomplete media for 24 h to attain the quiescent stage. The Boc-Pentagastrin and the antagonists were then added in incomplete media. The MTT assay was carried out after 48-120h of incubation by replacing fresh media and same concentration of Boc-Pentagastrin and/or the antagonist every day. The absorbance was measured as described above.

Conclusions

To summarize, the quinazolinone ring system has been employed as a template for the synthesis of two series of CCK-BR antagonists. The study resulted in development of potent CCK-BR antagonists. All the compounds were predicted for activities using pharmacophore mapping exercise and a good correlation was found between the experimentally determined and predicted antagonistic activities. The compounds showed favorable interactions within the binding site of homology modeled CCK-BR structure. Two best compounds **3c** and **4a** exhibited remarkable antagonistic activities of 0.2 nM and 17.36 nM respectively. The compounds also showed promising results in a functional gastric acid secretion assay using lumen-perfused isolated mouse stomach assay and inhibited growth of pancreatic cancer cells (MiaPaca-2) exhibiting good Cytotoxicity resulting in the most active compounds **3f** (hydrazine thiocarboxamide linker) and **4b** (hydrazine linker, indanone series). The compound **3f** being the best overall compound exhibiting good receptor binding affinity and cytotoxicity activity. Thus the optimized compounds in this study can be taken further for pre-clinical evaluation in drug discovery process to develop anticancer compounds against pancreatic cancer.

Acknowledgements

This work was supported by Department of Science and Technology (DST), Government of India and Department of Biotechnology (DBT), Government of India for providing Bioinformatics Facility at ACBR.

Conflict of Interest

The authors declare co competing interests.

Keywords:

Cholecystokinin Receptor Antagonist• Quinazolinone• Pancreatic Cancer • Biological activity • Molecular Modeling

References:

1 M. Hidalgo, *N. Engl. J. Med.*, 2010, **362**, 1605–1617.
2 R. Siegel, J. Ma, Z. Zou and A. Jemal, *CA Cancer J Clin*, 2014, **64**, 9–29.
3 D. P. Ryan, T. S. Hong and N. Bardeesy, *N. Engl. J. Med.*, 2014, **371**, 1039–1049.
4 L. Rahib, B. D. Smith, R. Aizenberg, A. B. Rosenzweig, J. M. Fleshman and L. M. Matrisian, *Cancer Res.*, 2014, **74**, 2913–2921.
5 J. P. Smith, C. A. Rickabaugh, P. J. McLaughlin and I. S. Zagon, *Am. J. Physiol.*, 1993, **265**, G149–155.
6 J. P. Smith, G. Liu, V. Soundararajan, P. J. McLaughlin and I. S. Zagon, *Am. J. Physiol.*, 1994, **266**, R277–283.
7 M. Dufresne, C. Seva and D. Fourmy, *Physiol. Rev.*, 2006, **86**, 805–847.
8 J. P. Smith, L. K. Fonkoua and T. W. Moody, *Int J Biol Sci*, 2016, **12**, 283–291.
9 J. P. Smith, J. F. Harms, G. L. Matters, C. O. McGovern, F. M. Ruggiero, J. Liao, K. K. Fino, E. E. Ortega, E. L. Gilius and J. A. Phillips, *Cancer Biol. Ther.*, 2012, **13**, 164–174.
10 M. R. Hellmich, X. L. Rui, H. L. Hellmich, R. Y. Fleming, B. M. Evers and C. M. Townsend, *J. Biol. Chem.*, 2000, **275**, 32122–32128.
11 J. P. Smith, W. B. Stanley, M. F. Verderame and I. S. Zagon, *Pancreas*, 2004, **29**, 271–277.
12 M. J. Berna and R. T. Jensen, *Curr Top Med Chem*, 2007, **7**, 1211–1231.
13 J. P. Smith, M. F. Verderame and I. S. Zagon, *Cancer Lett.*, 1999, **135**, 107–112.

14 S. A. Watson, D. Michaeli, S. Grimes, T. M. Morris, G. Robinson, A. Varro, T. A. Justin and J. D. Hardcastle, *Cancer Res.*, 1996, **56**, 880–885.
15 J. L. Abbruzzese, C. F. Gholson, K. Daugherty, E. Larson, R. DuBrow, R. Berlin and B. Levin, *Pancreas*, 1992, **7**, 165–171.
16 R. S. Chang, V. J. Lotti, T. B. Chen and K. A. Kunkel, *Mol. Pharmacol.*, 1986, **30**, 212–217.
17 R. Fossmark, Ø. Sørdal, C. S. Jianu, G. Qvigstad, I. S. Nordrum, M. Boyce and H. L. Waldum, *Aliment. Pharmacol. Ther.*, 2012, **36**, 1067–1075.
18 T. Meyer, M. E. Caplin, D. H. Palmer, J. W. Valle, M. Larvin, J. S. Waters, F. Coxon, I. Borbath, M. Peeters, E. Nagano and H. Kato, *Eur. J. Cancer*, 2010, **46**, 526–533.
19 G. A. Clawson, T. Abraham, W. Pan, X. Tang, S. S. Linton, C. O. McGovern, W. S. Loc, J. P. Smith, P. J. Butler, M. Kester, J. H. Adair and G. L. Matters, *Nucleic Acid Therapeutics*, 2016, **27**, 23–35.
20 J. P. Smith, S. Nadella and N. Osborne, *Cellular and Molecular Gastroenterology and Hepatology*, , DOI:10.1016/j.jcmgh.2017.03.004.
21 R. Herranz, *Med. Res. Rev.*, 2003, **23**, 559–605.
22 A. de Weerth, T. von Schrenck, M. Gronewold, F. Freudenberg, S. Mirau, M. Schulz and H. Greten, *Biochim. Biophys. Acta*, 1997, **1327**, 213–221.
23 S. Kumari, J. Chowdhury, A. K. Mishra, S. Chandna, D. Saluja and M. Chopra, *Chembiochem*, 2012, **13**, 282–292.
24 S. Kumari, N. Kalra, P. Mishra, K. Chutani, A. Mishra and M. Chopra, *Nuclear Medicine and Biology*, 2004, **31**, 1087–1095.
25 M. Chopra and A. K. Mishra, *J Chem Inf Model*, 2005, **45**, 1934–1942.
26 G. Semple, H. Ryder, D. P. Rooker, A. R. Batt, D. A. Kendrick, M. Szelke, M. Ohta, M. Satoh, A. Nishida, S. Akuzawa and K. Miyata, *J. Med. Chem.*, 1997, **40**, 331–341.
27 G. S. Baldwin, *Proceedings of the National Academy of Sciences of the United States of America*, 1994, **91**, 7593–7597.
28 N. Eswar, B. Webb, M. A. Marti-Renom, M. s. Madhusudhan, D. Eramian, M. Shen, U. Pieper and A. Sali, in *Current Protocols in Bioinformatics*, John Wiley & Sons, Inc., 2002.
29 M. Foucaud, I. G. Tikhonova, I. Langer, C. Escrieut, M. Dufresne, C. Seva, B. Maigret and D. Fourmy, *Mol. Pharmacol.*, 2006, **69**, 680–690.
30 R. Magnan, C. Escrieut, V. Gigoux, K. De, P. Clerc, F. Niu, J. Azema, B. Masri, A. Cordomi, M. Baltas, I. G. Tikhonova and D. Fourmy, *J. Am. Chem. Soc.*, 2013, **135**, 2560–2573.
31 M. J. Berna, J. A. Tapia, V. Sancho and R. T. Jensen, *Curr Opin Pharmacol*, 2007, **7**, 583–592.
32 T. Mosmann, *J. Immunol. Methods*, 1983, **65**, 55–63.
33 J. P. Smith, S. T. Kramer and T. E. Solomon, *Regul. Pept.*, 1991, **32**, 341–349.
34 J. P. Smith, A. P. Fantaskey, G. Liu and I. S. Zagon, *Am. J. Physiol.*, 1995, **268**, R135–141.
35 J. P. Smith, M. F. Verderame, P. McLaughlin, M. Martenis, E. Ballard and I. S. Zagon, *Int. J. Mol. Med.*, 2002, **10**, 689–694.
36 *Nucleic Acids Res*, 2015, **43**, D204–D212.
37V.-P. Jaakola, M. T. Griffith, M. A. Hanson, V. Cherezov, E. Y. T. Chien, J. R. Lane, A. P. Ijzerman and R. C. Stevens, *Science*, 2008, **322**, 1211–1217.
38 L. J. Miller and F. Gao, *Pharmacol. Ther.*, 2008, **119**, 83–95.
39 F. Noble, S. A. Wank, J. N. Crawley, J. Bradwejn, K. B. Seroogy, M. Hamon and B. P. Roques, *Pharmacol Rev*, 1999, **51**, 745–781.
40 H. J. C. Berendsen, D. van der Spoel and R. van Drunen, *Computer Physics Communications*, 1995, **91**, 43–56.
41 A. Cordomí, G. Caltabiano and L. Pardo, *J Chem Theory Comput*, 2012, **8**, 948–958.
42 M. Christen, P. H. Hünenberger, D. Bakowies, R. Baron, R. Bürgi, D. P. Geerke, T. N. Heinz, M. A. Kastenholz, V. Kräutler, C. Oostenbrink, C. Peter, D. Trzesniak and W. F. van Gunsteren, *J Comput Chem*, 2005, **26**, 1719–1751.
43 M. Parrinello and A. Rahman, *Journal of Applied Physics*, 1981, **52**, 7182–7190.
44 H. J. C. Berendsen, J. P. M. Postma, W. F. van Gunsteren, A. DiNola and J. R. Haak, *The Journal of Chemical Physics*, 1984, **81**, 3684–3690.
45 S. Nosé, *The Journal of Chemical Physics*, 1984, **81**, 511–519.
46 T. Darden, D. York and L. Pedersen, *The Journal of Chemical Physics*, 1993, **98**, 10089–10092.
47 B. Hess, H. Bekker, H. J. C. Berendsen and J. G. E. M. Fraaije, *J. Comput. Chem.*, 1997, **18**, 1463–1472.
48 R. Laskowski, M. Macarthur, D. Moss and J. Thornton, *J. Appl. Cryst.*, 1993, **26**, 283–291.
49 J. U. Bowie, R. Lüthy and D. Eisenberg, *Science*, 1991, **253**, 164–170.
50 C. Colovos and T. O. Yeates, *Protein Sci*, 1993, **2**, 1511–1519.
51 C. Ramakrishnan and G. N. Ramachandran, *Biophys J*, 1965, **5**, 909–933.
52 R. A. Laskowski, *Nucleic Acids Res*, 2001, **29**, 221–222.
53 J. K. Padia, M. Field, J. Hinton, K. Meecham, J. Pablo, R. Pinnock, B. D. Roth, L. Singh, N. Suman-Chauhan, B. K. Trivedi and L. Webdale, *J. Med. Chem.*, 1998, **41**, 1042–1049.
54 J. W. Black, P. Leff and N. P. Shankley, *Br. J. Pharmacol.*, 1985, **86**, 581–587.

View Article Online
DOI: 10.1039/C7MD00171A